Column base connections under compression and biaxial moments: proposed design approach

[a]R Cloete and [a]CP Roth*

[a]Department of Civil Engineering, University of Pretoria, Pretoria, 0002, South Africa

Tel: +2712 420 2185

* Corresponding author. Email: chris.roth@up.ac.za

HIGHLIGHTS

- A model is proposed for column base connections under compression and biaxial bending.
- The model utilises the plastic capacity of the plate on both sides of the connection.
- The model was compared to experiment and predicts behaviour fairly accurately.
- A linear moment interaction action equation is a conservative approach to design.

GRAPHICAL ABSTRACT

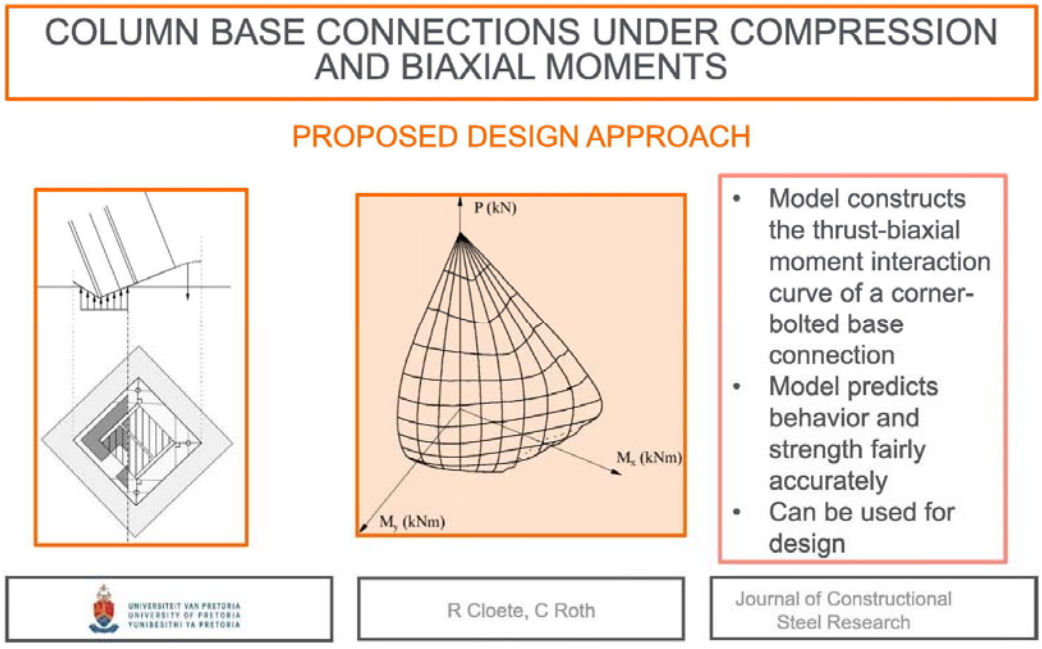

ABSTRACT

Very little guidance exists on the design of steel column base connections subjected to axial compression and biaxial bending. A new mechanical model is proposed here for designing such base connections. The model constructs the thrust-moment interaction curve of the connection, which can then be used for design. The method is aimed at unstiffened baseplates with four corner bolts, but may readily be extended to other layouts. The model makes several simplifying assumptions that reduces the problem to 3 modes of failure that employ simple geometric expressions and statics to calculate bolt and prying forces. Contrary to the Eurocode and AISC approach, the proposed model utilises the full plastic capacity of the plate under all loading conditions and on both the tension and compression sides of the connection. The resulting interaction curves were compared to experimental results from an experimental program of thirty-two tests to failure. The model predicts behaviour fairly accurately. It was also shown that the use of a linear moment interaction action equation is a conservative approach to designing base connections for axial force and biaxial bending.

Keywords: column baseplate, biaxial bending, design approach, T-stub

1. INTRODUCTION

A steel column base connection is a complex connection that may be used to transfer axial and shear forces, torsion and biaxial moments from a column safely into a footing. The connection includes several components such as steel baseplate, concrete footing, and steel holding down (HD) bolts; and has interfaces between the various elements. The connection is often required to transfer axial compression and uniaxial bending, but the combination of axial compression and biaxial bending may also be important.

Several design guidelines are available, such as AISC 360 [1] along with the *Steel Design Guide Series 1* [2] and EN 1993 [3] along with *Moment-Resisting Joints to Eurocode 3* [4]. These describe uniaxial bending with axial force and shear, but guidance on design for biaxial bending situations, with and without axial forces, has been absent from design approaches in the United States, Europe and elsewhere. Only recently have limited attempts been made to remedy this lack. The South African Institute of Steel Construction Green Book [5] that accompanies the South African standard for hot-rolled steelwork SANS 10162 [6] proposes a design approach but neglects the effect that plate stiffness has on the distribution and magnitude of concrete contact stresses. Amaral [7] proposed an elliptical interaction surface based on a limited number of tests and numerical results.

This paper proposes a design method for column baseplates under axial force and biaxial bending. The method is aimed at unstiffened baseplates with four corner HD bolts as shown in Figure 1, but may readily be extended to other layouts.

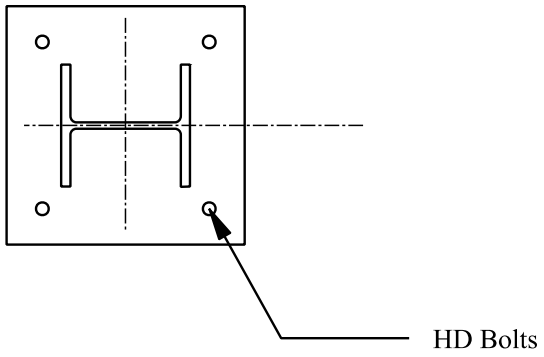

Figure 1: Typical baseplate with four corner bolts

Recently, data has become available from an experimental program of thirty-two tests to failure that was carried out to determine the effects of various factors that affect the strength and behavior of such baseplate connections [8,9]. Plate thickness, HD bolt diameter and axial compression were set to low and high values in a full factorial experimental design chosen to bring about different failure modes. The investigations gave a clearer understanding of the behaviour of baseplates under biaxial bending, and will be used to check results from the proposed design method.

Comparisons of the new model's predictions to other experimental work on biaxial loading is hampered by the scarcity of results in the available literature. The only papers on this topic that were reviewed [7, 10] focussed on bolt layouts that are outside the immediate scope of the proposed method.

Authors that have proposed design methods for uniaxial flexure with or without axial force include the following. Drake and Elkin [11] presented a method for designing column base plate connections that is consistent with limit state principles. With a few modifications suggested in a discussion of the paper [12], this is the method used in [2]. Stamatopoulos and Ermopoulos [13] presented a method for constructing axial force-moment interaction diagrams based on statics and from these equations interaction diagrams can be constructed for given connection geometries. The authors compared the predictions of their model with

experimental work from other researchers and found better agreement than with the EN 1993 model. Lee and co-workers reported on an investigation into the behaviour of column base connections subjected to weak axis flexure in the absence of axial load [14,15,16]. Several limitations of the Drake and Elkin design method were emphasised and a new design method that is based on a simple beam analogy was outlined that offered an improved description of the behaviour of base connections in weak axis bending when compared to the DE method. Gomez at al. [17] reported on an experimental programme that investigated the response of base connections and found that the strength predictions of [2] were very conservative in all cases and proposed that the design method should be modified.

2. PROPOSED DESIGN APPROACH

The methods described in section 1 all proceed by analogy to reinforced concrete design where the HD bolts serve as tension reinforcement and the effective area under the column correlates with a concrete stress block. The analogy is sound, but suffers from the lack of a known strain distribution at concrete failure which determines steel stresses. In the uniaxial case, where all the steel is at a single distance from the neutral axis, one can simply assume that the HD bolts in tension are stressed to capacity and that the connection possesses sufficient ductility to ensure that this is the case.

However, under biaxial flexure the neutral axis is inclined to the bolt layout and some HD bolts may be on, or near, the neutral axis and consequently at a much lower stress than the bolt with the largest lever arm. The assumption that all the bolts are at the yield stress cannot be justified in the light of the extreme rotations that would be required to achieve this. Furthermore, an assumption that only the highest stressed HD bolt provides resistance would be excessively conservative.

The objection of unrealistically large rotations applies to both uniaxial and biaxial loading combined with high axial load, as it is highly improbable that a connection with a very deep neutral axis would be able to sustain rotations of sufficient magnitude to yield the HD bolts. Without information on the failure strain or displacement at concrete bearing failure, some limiting value for the maximum permissible connection rotation should be part of the model.

The proposed mechanical model makes four simplifying assumptions:

1. The rectangular area that encloses the column section remains rigid and rotates about the neutral axis. This assumption can be justified by noting that the in-plane stiffness of the flanges and web is extremely high and, assuming negligible column section warping, the column section remains plane.

2. The rotation magnitude is limited by the fracture strain of the HD bolt with the largest lever arm. Stress distribution between the HD bolts requires a connection rotation and the fracture strain seems to be a sensible limit. Early brittle concrete failure remains a concern that cannot be addressed here, but the model does support a further rotation limit that has been set to 0.2 radians, twice the maximum recorded in the experimental work described in [8]. Conservatism inherent in the concrete strength calculation [18,19] allays this concern somewhat.

3. The plate can be partitioned into four independent quadrants and each of these quadrants can be replaced with an effective beam spanning from a flange edge through the bolt centre to the plate edge. The model will only be validated against the corner-bolted connections studied in this work, but it should readily extend to different four-bolt layouts.

4. Yield lines in these four quadrants are orthogonal to the line connecting the flange tip and HD-bolt and are located at the flange tip and bolt centres. Note that the yield line

orientation is a function of geometry only. Yield lines terminate at the plate edge or quadrant boundary.

The main features of these assumptions are illustrated in Figure 2. Based on these assumptions a modified T-stub approach is used to determine the capacity of each corner for a given neutral axis position and orientation. By varying the neutral axis rotation and depth, the full thrust-moment interaction surface at a particular maximum rotation can be constructed.

Unlike in the AISC and Eurocode design approaches, the model does not use compression side plate yielding as a failure criterion. As noted in Gomez [20], plate yielding on the compression side alone is not sufficient to form a plastic mechanism and should not be used as a failure criterion.

It can be seen from Figure 2 that the approach described in this work limits the neutral axis depth to the extents of the rigid column area. The mechanical model does thus not include the behaviour of very thick plates where the column is not in contact with the concrete surface and in the case of very deep neutral axes, the HD bolts are assumed inactive.

Design of the weld connecting the column and baseplate is beyond the scope of the method, and it is assumed that the welds have sufficient strength. As noted in [8], the welds at the flange tips of corner bolted base connections under biaxial bending are vulnerable to premature failure and it may be prudent to prescribe some form of penetration weld in these cases. Further research is needed in this area.

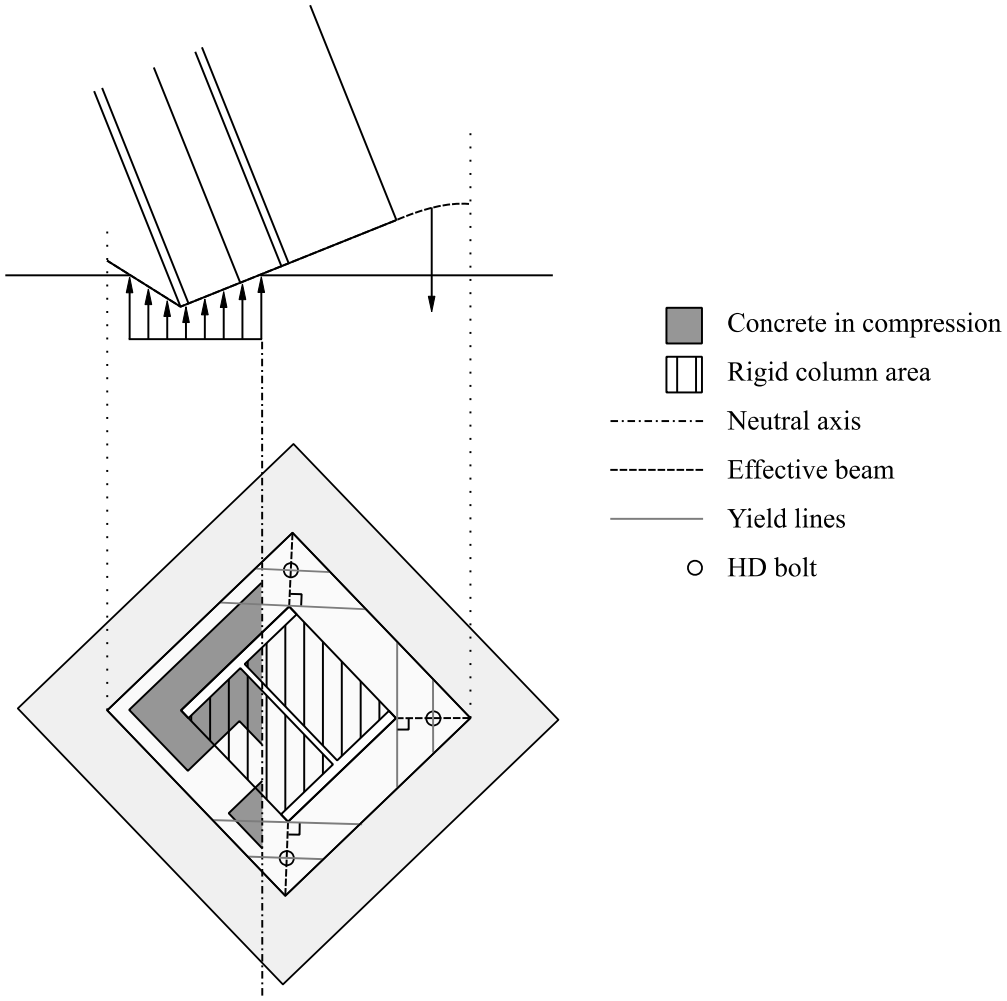

Figure 2: Core assumptions of the mechanical model

2.1 MODIFIED T-STUB FOR BASEPLATE

The T-stub approach [21] assesses the effect of prying actions on end-plates and bolts. In this section a modification of the T-stub approach is employed to calculate bolt and prying forces due to a known rotation of the rigid column area. The exposition below was inspired in part by the work of Wheeler et al [22]. Three modes of failure are considered in the following sections and the variables used are shown in Figure 3. The seemingly reverse order of the sections below is caused by a desire to remain consistent with existing terminology used for the modes of connection failure.

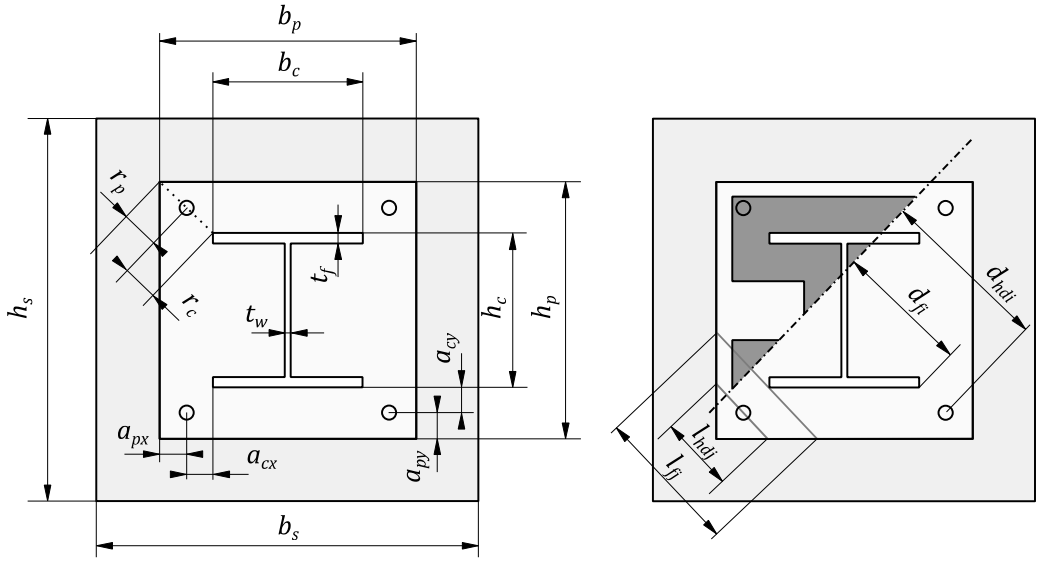

Figure 3: Model geometry and dimensions

The plastic moment capacities of the effective beam at the flange tip and bolt position are required in order to delineate the boundaries between the T-stub failure modes. The plastic moment capacity per unit width is given by equation 1.

$$m_p = \frac{1}{4} f_{pp} t_p^2 \tag{1}$$

where:

m_p = plastic moment capacity per unit width

t_p = plate thickness

f_{pp} = plate design stress

Due to the large relative plate rotations inherent in plastic collapse mechanisms, significant strain hardening occurs. It was found that by using a design stress that includes an allowance for strain hardening [23], also used in [22], a much closer fit with experimental results could be achieved. This design stress can be calculated with equation 2.

$$f_{pp} = \frac{f_{yp} + 2f_{up}}{3} \tag{2}$$

where:

f_{yp} = plate yield stress

f_{up} = plate ultimate tensile strength

The total moment capacities at the flange tip and HD bolt are given by equations 3 and 4.

$$M_{pfi} = m_p l_{fi} \tag{3}$$

$$M_{phdi} = m_p l_{hdi} \tag{4}$$

where:

M_{pfi} = plastic moment capacity at the flange tip i

l_{fi} = yield line length at flange tip i

M_{phdi} = plastic moment capacity at the HD bolt i

l_{hdi} = yield line length at HD bolt i

Values for l_{fi} and l_{hdi} can be calculated from simple geometry given the plate dimensions and bolt layout.

2.1.1 Failure mode 3

Thick, stiff plates fall into this category of failure. It is assumed that the moment at the bolt and flange positions are both below the respective plastic moments. The force in the bolt then follows from the assumed connection rotation and the geometry as shown in Figure 4. The treatment below is broadly similar to the approach followed by others [24] for calculating the uniaxial moment-rotation response of base connections.

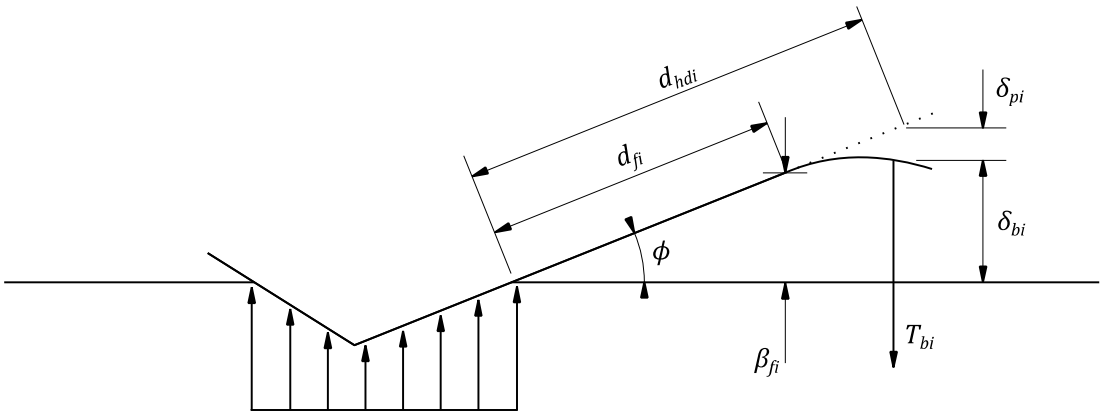

Figure 4: Failure mode 3

The displacement at flange tip i, β_{fi}, can be calculated quite simply by employing the small angle approximations as shown in equation 5.

$$\beta_{fi} = d_{fi}\phi \tag{5}$$

The displacement of the plate, δ_{pi}, and bolt, δ_{bi}, follow from equations 6 and 7. Equation 6 is the displacement of a cantilever beam subjected to a point load and equation 7 is the displacement of an axially loaded rod.

$$\delta_{pi} = \frac{T_{bi} r_c^3}{3 E_s I_p} \tag{6}$$

$$\delta_{bi} = \frac{T_{bi} L_b}{A_b E_s} \tag{7}$$

$$I_p = \frac{(l_{fi} + l_{hdi}) t_p^3}{24} \tag{8}$$

where:

r_c = distance from the flange tip to the bolt centre

E_s = steel modulus of elasticity

T_{bi} = force in HD bolt i

I_p = average of the moments of inertia at l_{fi} and l_{hdi}

L_b = strained length of the HD bolt

A_b = cross-sectional area of HD bolt

Based on the results of the bond tests in [9] and finite element simulations in [8] and [9], it was determined that the strained length of the HD bolts should be equal to the entire embedded length up to the anchor plate. Furthermore, the moment of inertia used for the effective beam is a simplification that is only exact for strong or weak axis bending. Order of magnitude changes to the moment of inertia had very little effect on the calculated capacities and thus a more rigorous treatment cannot be justified.

From similar triangles,

$$\frac{\beta_{fi}}{d_{fi}} = \frac{\delta_{pi} + \delta_{bi}}{d_{hdi}} \tag{9}$$

and inserting equations 6 and 7,

$$\frac{\beta_{fi}}{d_{fi}} = \frac{T_{bi}}{d_{hdi}}\left(\frac{r_c^3}{3E_s I_p} + \frac{L_b}{A_b E_s}\right) \tag{10}$$

After rearranging terms, it follows that the bolt force can be calculated by using equation 11.

$$T_{bi} = \beta_{fi}\frac{d_{hdi}}{d_{fi}}\left(\frac{3A_b E_s I_p}{3I_p L_b + A_b r_c^3}\right) \leq f_{pb} A_b \tag{11}$$

where:

f_{pb} = HD bolt design stress, calculated on the same basis as shown in equation 2.

If T_{bi} exceeds the value required for the moment at the flange tip to reach M_{pfi}, as shown in equation 12, failure mode 3 is impossible and thus failure mode 2 should be checked.

$$T_{bi} \leq \frac{M_{pfi}}{r_c} \tag{12}$$

2.1.2 Failure mode 2

Failure mode 2, shown in Figure 5, occurs with plates of intermediate thickness. In this failure mode, a yield line forms at the flange tip, but the geometry is such that the moment at the bolt position is not yet fully plastic. The yield line at the flange tip forms a plastic hinge and permits treatment of the plate as a simply-supported beam.

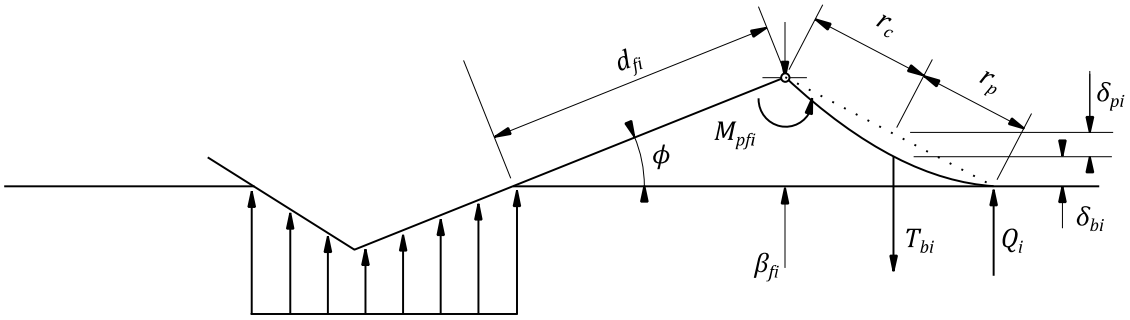

Figure 5: Failure mode 2

The flange tip and bolt displacements can again be calculated with equations 5 and 7, but the plate displacement now follows from equation 13, which is the equation for calculating the displacement of a simply supported beam subjected to a point load.

$$\delta_{pi} = \frac{T_{bi} r_p^2 r_c^2}{3(r_p + r_c) E_s I_p} \tag{13}$$

Similar triangles are again employed,

$$\frac{\beta_{fi}}{r_p + r_c} = \frac{\delta_{pi} + \delta_{bi}}{r_p} \tag{14}$$

and after inserting equations 7 and 13,

$$\frac{\beta_{fi}}{r_p + r_c} = \frac{T_{bi}}{r_p}\left(\frac{r_p^2 r_c^2}{3(r_p + r_c) E_s I_p} + \frac{L_b}{A_b E_s}\right) \tag{15}$$

After rearranging terms, the bolt forces can be calculated with equation 16. Prying forces follow from moment equilibrium at the flange tip as shown in equation 17.

$$T_{bi} = \beta_{fi} \frac{r_p}{r_p + r_c}\left(\frac{L_b}{A_b E_s} + \frac{r_p^2 r_c^2}{3(r_p + r_c) E_s I_p}\right)^{-1} \leq f_{pb} A_b \tag{16}$$

$$Q_i = \frac{T_{bi} r_c - M_{pfi}}{r_p + r_c} \leq Q_{maxi} \tag{17}$$

where:

Q_{maxi} = maximum possible prying force at bolt *i* as defined in the next section

If Q_i exceeds Q_{maxi}, then mode 2 cannot occur and mode 1 needs to be checked.

2.1.3 Failure mode 1

Failure mode 2 above involves contact with the concrete at the plate edge where the prying force, Q_i, increases from zero to a value that causes plate yielding at the bolt position. This two-hinge mechanism then constitutes a mode 1 failure, shown in Figure 6, in which the prying force is at its maximum value.

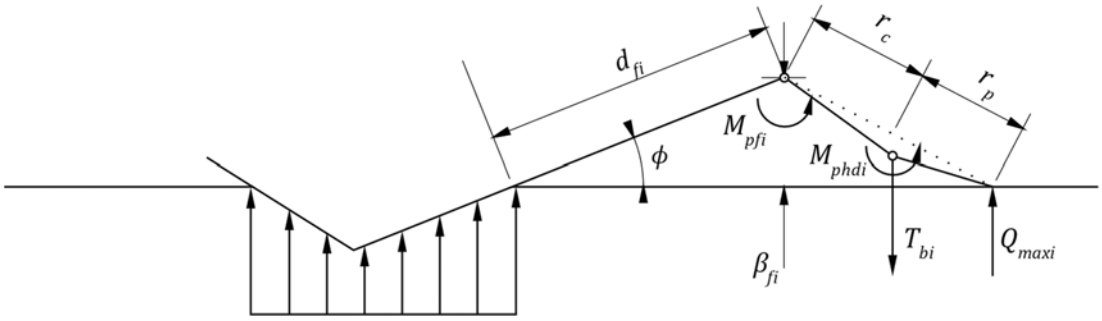

Figure 6: Failure mode 1

The maximum prying force in this configuration is expressed by equation 18.

$$Q_{maxi} = \frac{M_{phdi}}{r_p} \tag{18}$$

Rearrangement of equation 17 yields the bolt force as shown in equation 19.

$$T_{bi} = \frac{Q_i(r_p + r_c) + M_{pfi}}{r_c} \leq f_{pb}A_b \tag{19}$$

2.2 CONCRETE RESISTANCE

Although concrete damage was observed during the experiments described in [8], barring a single test, no failure occurred in which concrete bearing failure governed the behaviour. Nevertheless, concrete failure must form part of a design method and a modification of current South African practice [5], which is similar to EN 1993 [3], is suggested.

The concrete area in compression is assumed, as is current practice, to extend beyond the column flange and web by a cantilever distance given by equation 20.

$$c = t_p\sqrt{\frac{f_y}{2f_{br}}} \tag{20}$$

The bearing strength is expressed by equation 21.

$$f_{br} = f_{ck}\sqrt{\frac{A_2}{A_1}} \tag{21}$$

where:

f_{ck} = measure of concrete strength, currently cube strength.

The research upon which equation 21 is based involved tests that loaded concrete blocks with a rigid rectangular punch, and thus it seems inappropriate to use T or I-shaped areas such as those shown in Figure 3.

It is proposed then that A_1 be based on the rectangular area that encloses the entire column, in effect, the same rigid area shown in Figure 1 and A_2 should be an area of concrete congruent with A_1, as shown in Figure 7. Note that this approach may lead to overly conservative estimates of concrete bearing strength when very deep sections are used.

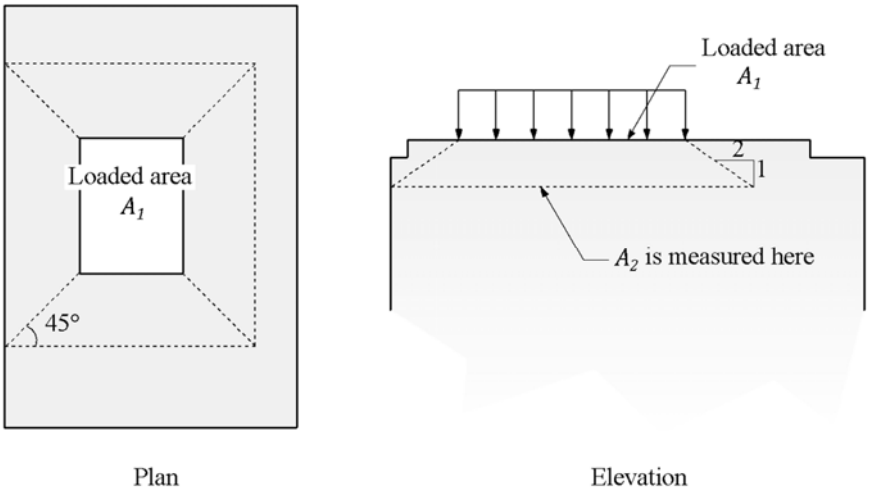

Figure 7: Finding A_2 for stepped or sloped supports and non-concentric loading, sketch adapted from ACI 318 [25]

With these definitions, the bearing strength becomes a function of the cantilever distance as shown in equation 22 and the cantilever distance becomes an iterative calculation.

$$f_{br} = f_{ck}\sqrt{\frac{A_2}{(b_c + 2c)(h_c + 2c)}} \tag{22}$$

2.3 INTERACTION SURFACE

Computer code was implemented in C++ to calculate the interaction surface using the model described in the previous section. The algorithm starts with the calculation of the polygon of the concrete surface in compression under pure axial compression. The angle of

the neutral axis is then varied from 0° to 90° and the neutral axis depth is in turn varied from one flange tip to the opposite flange tip within each angle increment. Figure 8 shows a diagram of the algorithm described above.

The calculation described above results in a set of space curves in M_x-M_y-P space as shown in Figure 9. The boundaries between the failure modes display as abrupt slope changes in the curves.

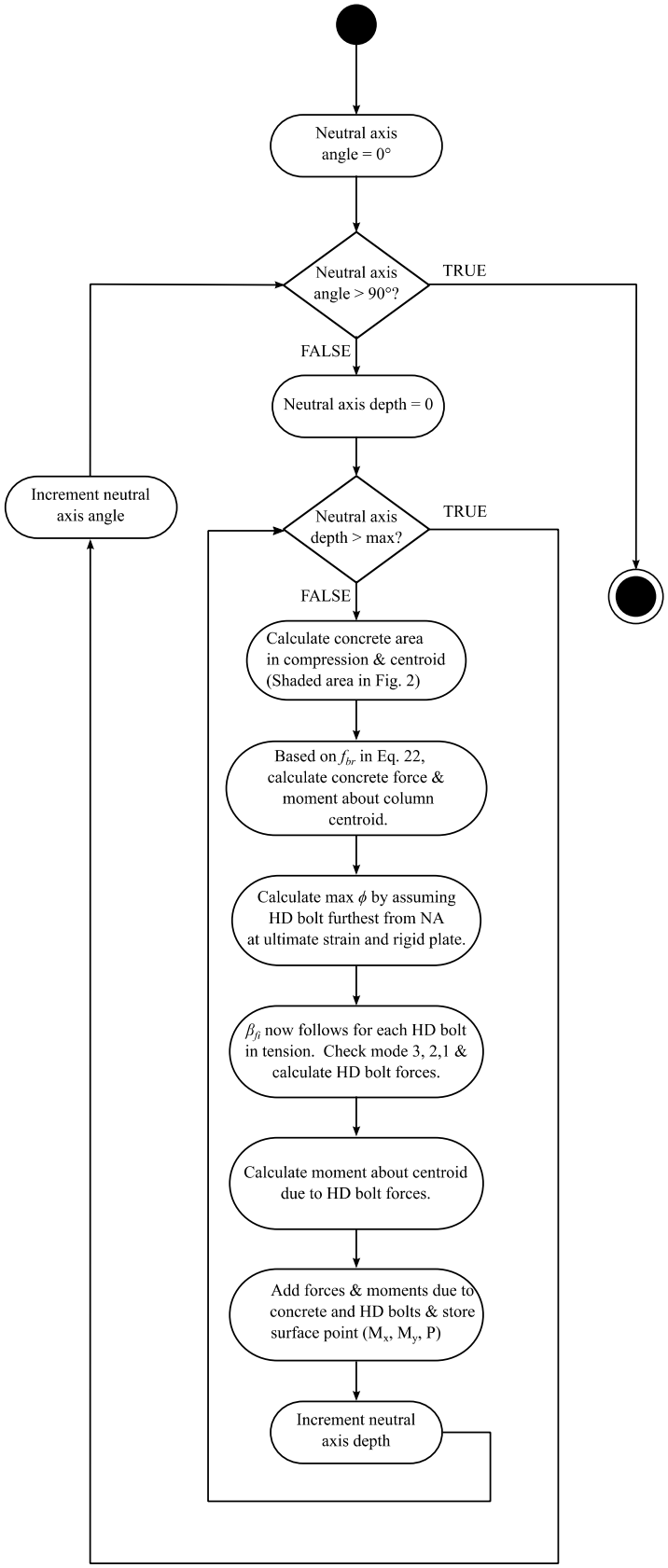

Figure 8: Diagram of the surface generation algorithm

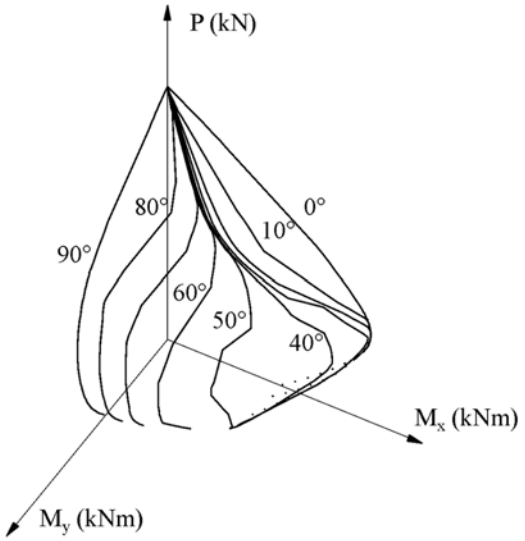

Figure 9: Failure surface

The neutral axis curves are unsuitable for design purposes since the neutral axis angle for any particular combination of loads is not known at the outset. Thus, the neutral axis curve values are interpolated at a range of axial force values and a set of moment contour curves are generated. These contours can be further post-processed by interpolation at fixed ratios of M_y to M_x and results in a set of curves that can be used directly for design purposes as shown in Figure 10.

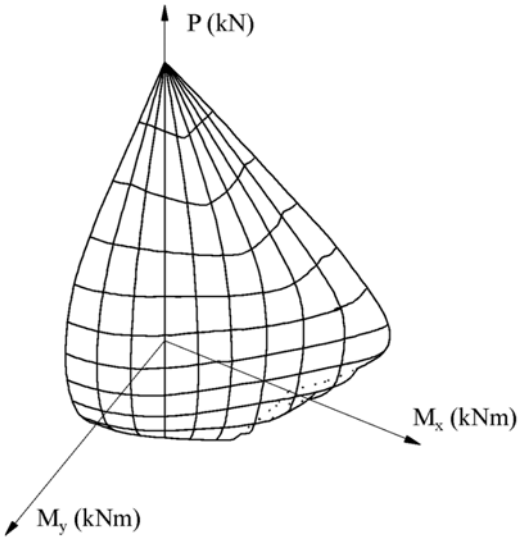

Figure 10: Regularised interaction surface curves

In order to use the method in routine design, entire failure surfaces can be constructed by computer for various HD bolt and plate combinations. Those for which the applied loads plot inside the surface can be identified, and the optimum solution can then be chosen based on cost and practical considerations such as minimum bolt size.

The interaction surface clearly shows that, at the cost of some conservatism, the approach can be simplified even further by the observation that the moment contours can be approximated with a line as shown in Figure 11. The design process would then consist of constructing the strong and weak-axis interaction curves and ensuring that the applied loads plot inside the curves in addition to satisfying equation 23. This type of equation is used in many design codes, for example for combined flexure and axial force.

$$\frac{M_x}{M_{rxp}} + \frac{M_y}{M_{ryp}} \leq 1 \tag{23}$$

where:

M_{rxp}= Moment resistance about the x-axis at the applied axial load.

M_{ryp}= Moment resistance about the y-axis at the applied axial load.

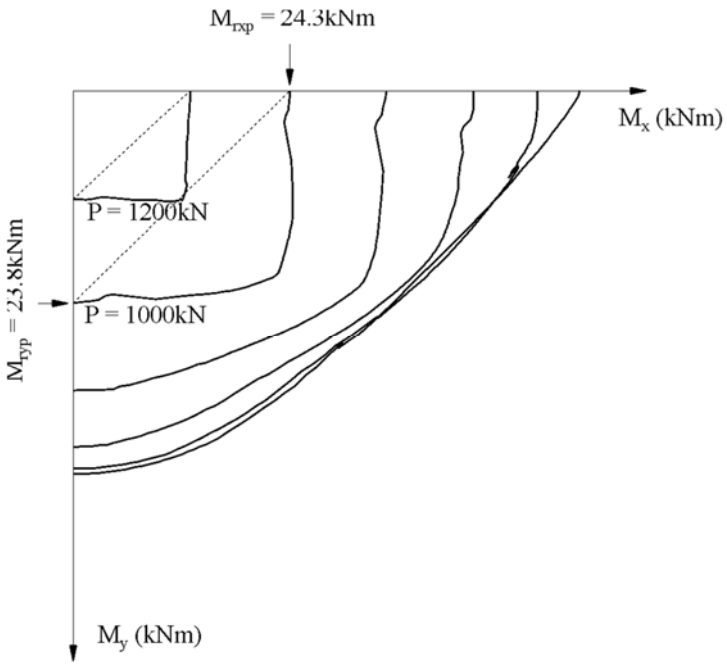

Figure 11: Typical moment contours

3. COMPARISON WITH TEST RESULTS

In this section, the capacity predicted by the proposed design approach will be compared to results of the extensive experimental programme of thirty-two tests of baseplate connections to failure. Details of the programme can be found in [8].

In the experiments, the plate thickness was varied between 10mm and 16mm; the HD bolt diameter between 16mm and 24mm; and the axial compression force between 0kN and 350kN. The parameters varied between the high and low values over 4 loading angles: 0° (strong axis bending), 30° (0.866 times the resultant moment about the strong axis and 0.5 times the resultant moment about the weak axis), 60° (0.5 times the resultant moment about the strong axis and 0.866 times the resultant moment about the weak axis) and 90° (weak axis bending) – thus providing information on connection behaviour at 2 uniaxial and 2 biaxial loading angles. The naming of the specimens followed the pattern: Angle-Plate thickness-Bolt diameter-Axial load, so for example 0-10-16-0 refers to a test with 0° loading angle, 10mm plate, 16mm HD bolt and 0kN axial load.

Results will be presented on interaction curves with the resultant moment on the horizontal axis. The connection interaction curve from the proposed design method will be shown, along with the plastic interaction curve of the column. The overall interaction curve, which is the minimum of the connection and column curves, will be shown using a thicker, grey line.

The various combinations of loading angle, baseplate thickness and HD bolt diameter are shown in Figures 11-14. On each graph two sets of results are shown, one with the 0kN axial force and one with the 350kN axial force. For example, Figure 11a) shows the results for the two axial forces for the samples with 0° loading angle, 10mm plate and 16mm HD bolt.

Figure 11 shows the results for 0° loading (strong axis bending). The connection interaction curve generally controls the capacity, except for higher axial loads in the 16mm

baseplate connections. The correspondence between predicted and observed capacities is fair, and overall behaviour is predicted well.

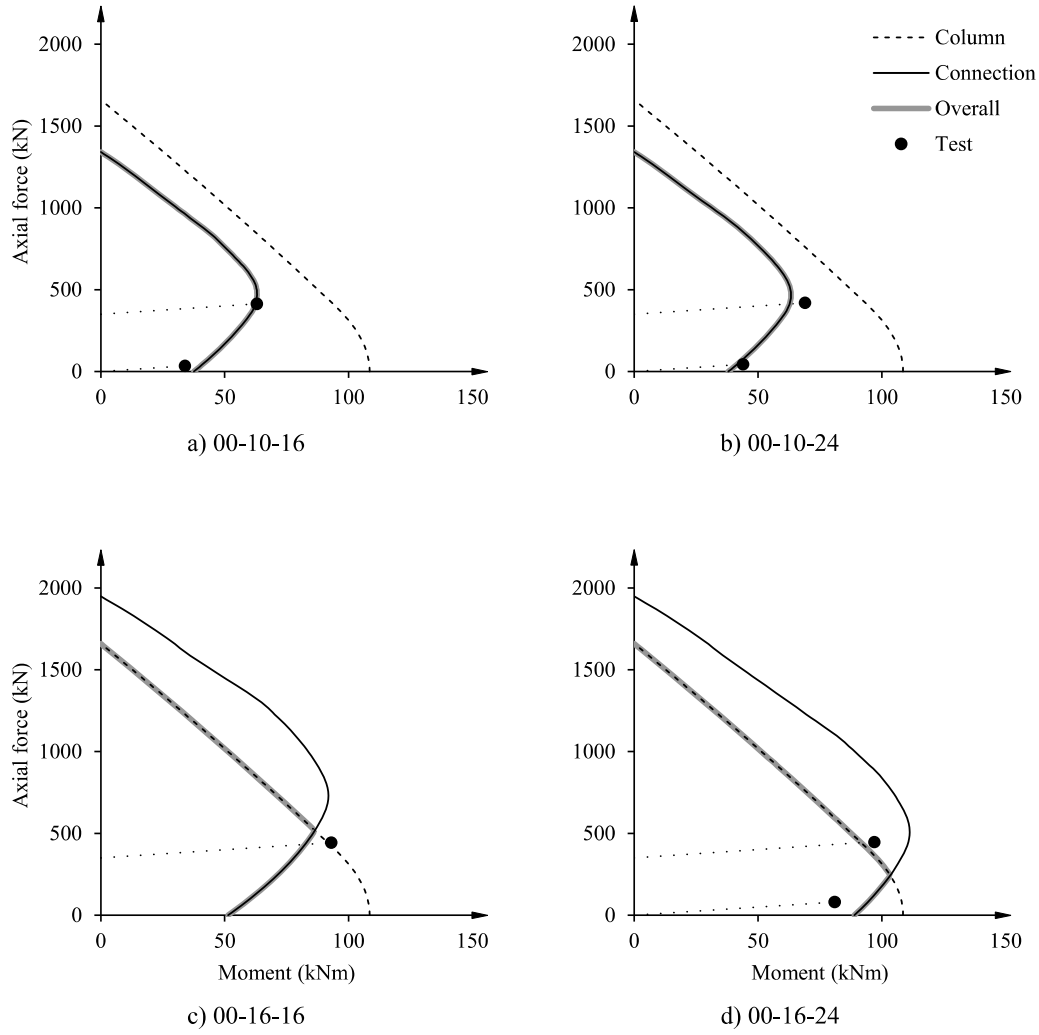

Figure 11: Interaction diagrams, 0° loading

Figure 12 shows the results for 30° loading. The correspondence between predicted and observed capacities is again fair, and overall behaviour is predicted well with the connection interaction curve generally controlling the capacity, except for higher axial loads in the 16mm baseplate connections.

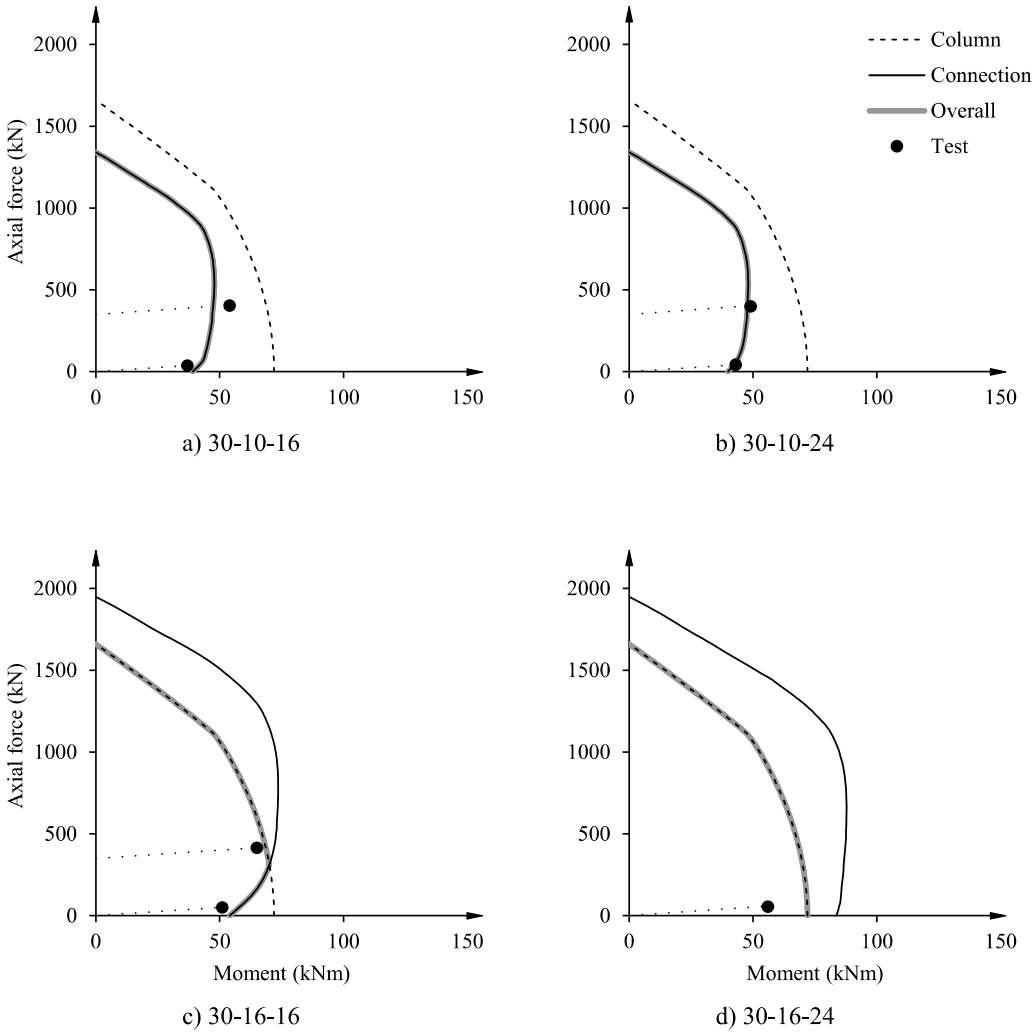

Figure 12: Interaction diagrams, 30° loading

Figure 13 shows the results for 60° loading. The correspondence between predicted and observed capacities is again fair.

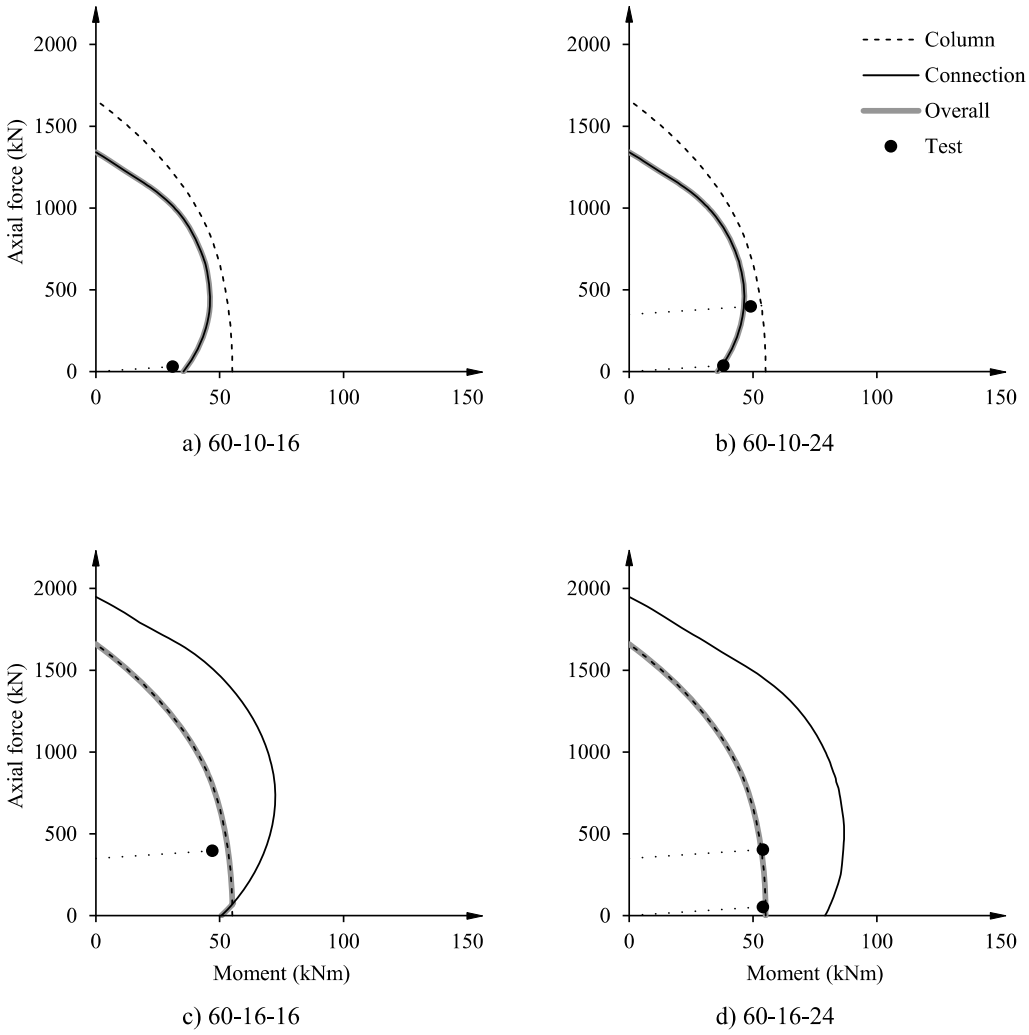

Figure 13: Interaction diagrams, 60° loading

Figure 14 shows the results for 90° loading (weak axis bending). The correspondence between predicted and observed capacities is again good. The tests with a 16mm baseplate were completely controlled by the column interaction curve.

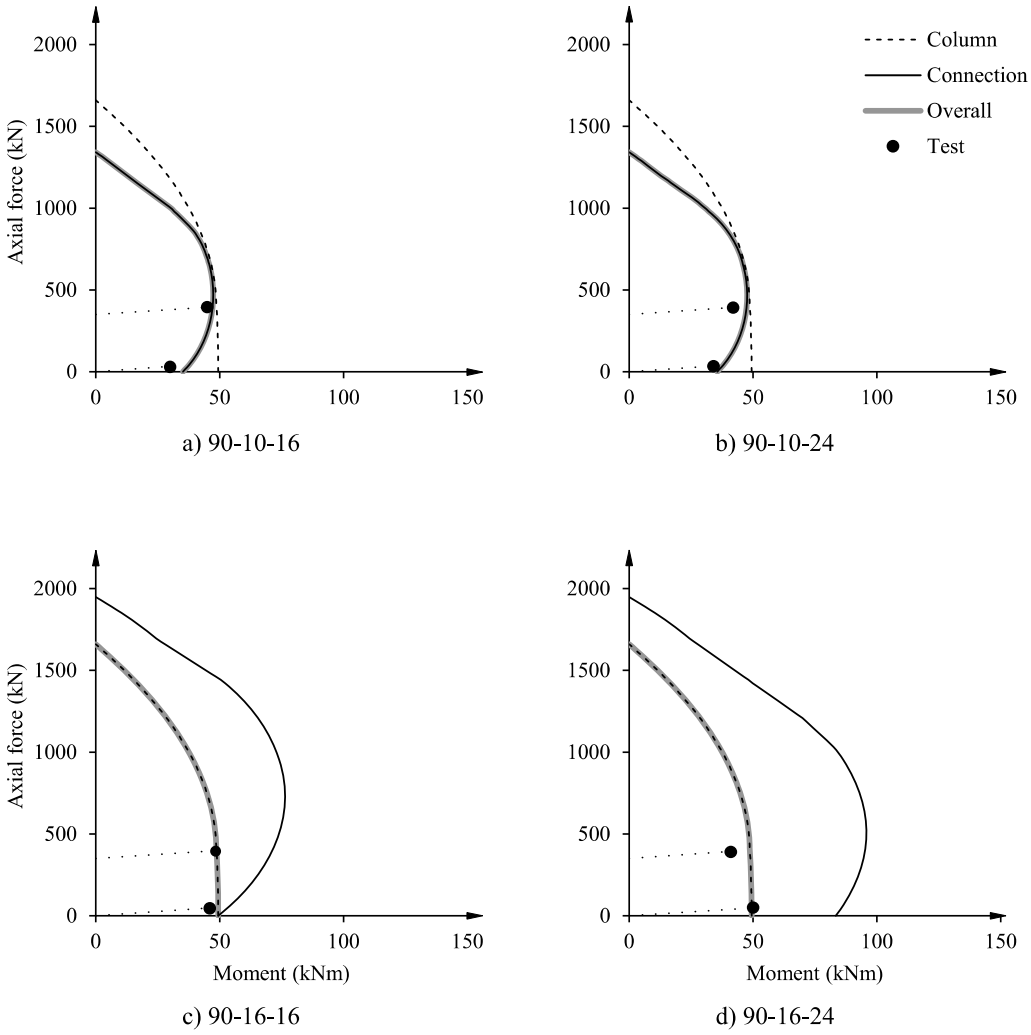

Figure 14: Interaction diagrams, 90° loading

Table 1 below summarises the results of the experimental programme compared to predictions from the proposed design approach. The cause of failure is indicated with the symbol ● and failures also noted with the symbol ○. The experimental results did not distinguish between Mode 1 and Mode 2 failures, so plate failure observed during a test was assigned to both modes.

Table 1: Summary

Designation (*Angle*-p*late*-b*olt*-a*xial*)	Result	Failure mode				Maximum moment (kNm)
		Mode 3	Mode 2	Mode 1	Column	
00-10-16-0	Test		●	●		34
	Design method		●			41
00-10-16-350	Test		●	●	●	63
	Design method		●			62
00-10-24-0	Test		●	●		44
	Design method			●		41
00-10-24-350	Test		●	●		69
	Design method			●		63
00-16-16-350	Test		●	●	○	93
	Design method	●				82
00-16-24-0	Test		●	●	○	81
	Design method		●			95
00-16-24-350	Test		●	●	●	97
	Design method		●			91
30-10-16-0	Test		●	●	○	37
	Design method		●			42
30-10-16-350	Test		●	●	○	56
	Design method		●			47
30-10-24-0	Test		●	●	○	44
	Design method			●		43
30-10-24-350	Test		●	●	○	49
	Design method			●		48
30-16-16-0	Test		●	●	○	51
	Design method	●				58
30-16-16-350	Test		○	○	○	65
	Design method				●	69
30-16-24-0	Test		●	●	○	57
	Design method				●	72
60-10-16-0	Test		●	●	○	32
	Design method		●			37
60-10-24-0	Test		●	●	○	38
	Design method			●		38
60-10-24-350	Test		○	○	○	49
	Design method			●		46
60-16-16-350	Test				●	47
	Design method				●	53
60-16-24-0	Test		●	●	○	54
	Design method				●	55
60-16-24-350	Test				●	55
	Design method				●	54
90-10-16-0	Test		●	●	○	31
	Design method		●			37
90-10-16-350	Test		●	●	●	45
	Design method		●			47
90-10-24-0	Test		●	●	○	34
	Design method			●		38
90-10-24-350	Test				●	42
	Design method			●		47
90-16-16-0	Test				●	46
	Design method				●	49

Table 1: Summary (continued)

Designation (*Angle*-p*late*-b*olt*-a*xial*)	Result	Failure mode				Maximum moment (kNm)
		Mode 3	Mode 2	Mode 1	Column	
90-16-16-350	Test				●	49
	Design method				●	49
90-16-24-0	Test				●	50
	Design method				●	49
90-16-24-350	Test				●	41
	Design method				●	49

The table summarises the results in Figures 11 to 14, and comparison of the moments in the right column clearly shows that the design method generally predicts the failure moment in the tests well. The failure mode is also correctly predicted in most cases. There are some discrepancies which can be explained. The differences in 0-10-16-0, 30-16-24-0, 60-10-16-0 and 90-10-16-0 are due to premature weld failures in the tests. As noted in section 2, the design method does not consider the weld, but assumes that it is strong enough. Some of the welds in the tests were undersized.

4. COMPARISON WITH EXISTING DESIGN APPROACHES FOR STRONG AXIS BENDING

As noted in the introduction, existing design codes do not make allowance for biaxial bending so the only direct comparisons can be made for uniaxial strong axis bending, the 0° series of tests. Comparisons are made here against the three current design codes listed in the introduction.

Table 2 shows the plate thickness and HD bolt diameter that would be required by the proposed design method and each of the three design codes considered to resist the various axial force and moment combinations. 00-16-24-350 is not included as column failure controls.

Table 2: Comparison of design approaches

Design method	Thickness (mm)	HD-bolt (mm)	Thickness (mm)	HD-bolt (mm)
	00-10-16-0 (P=40kN M_x=41kN.m)		**00-10-16-350 (P=403kN M_x=62kN.m)**	
Proposed method	10	16	10	16
AISC Design Guide 1	25	12	35	10
EN 1993	16	16	25	16
Green book	12	16	16	12
	00-10-24-0 (P=40kN M_x=41kN.m)		**00-10-24-350 (P=403kN M_x=62kN.m)**	
Proposed method	10	16	10	16
AISC Design Guide 1	25	12	35	10
EN 1993	16	16	25	16
Green book	12	16	16	12
	00-16-16-0 (P=58kN M_x=57kN.m)		**00-16-16-350 (P=429kN M_x=82kN.m)**	
Proposed method	16	16	16	16
AISC Design Guide 1	30	16	35	12
EN 1993	16	24	30	24
Green book	16	16	16	16
	00-16-24-0 (P=97kN M_x=95kN.m)			
Proposed method	16	24		
AISC Design Guide 1	35	24		
EN 1993	25	24		
Green book	20	24		

Although the emphasis here is not on uniaxial bending, the results show that for the uniaxial case the method can yield savings in plate thickness compared to the AISC and Eurocode methods.

5. CONCLUSIONS

A new model was proposed to construct the thrust-moment interaction curve of a corner-bolted base connection, which can then be used for design. The model makes several simplifying assumptions that reduces the problem to three modes of failure that employ simple expressions to calculate bolt and prying forces. The resulting interaction curves were compared to experimental results. The model predicts behaviour fairly accurately.

The model should be readily extensible to other bolt layouts and in fact, reduces to the classical one-sided T-stub failure when the bolts align with the flange tips. Section shapes such as rectangular hollow sections can be used without modification, but some care may be required with very deep I-shaped sections. Stiffeners effectively extend the assumed rigid area and should not pose any problems either.

Contrary to the Eurocode and AISC approach, the proposed model utilises the full plastic capacity of the plate under all loading conditions and on both the tension and compression sides of the connection. As noted above, this approach leads to much better results than using compression side yielding as a failure criterion. The proposed model also improves on the AISC approach in particular by providing a prediction of the connection capacity, and it would therefore be especially useful in evaluating the strength of existing connections. Finally, the proposed model remedies the neglect of HD bolt layout effects in the AISC approach, as noted by Lee et al. [14].

It has been shown that the use of a linear moment interaction action equation, equation 23, is a conservative approach to designing base connections for biaxial loading. This approach can be used if a conservative result is acceptable, and can be considered for inclusion in a design code.

ACKNOWLEDGEMENTS

This research did not receive any specific grant from funding agencies in the public, commercial, or not-for-profit sectors. The assistance of the South African Institute of Steel Construction is acknowledged.

REFERENCES

[1] AISC, Specification for Structural Steel Buildings, American Institute of Steel Construction, Chicago, 2005.

[2] J.M. Fisher, L.A. Kloiber, Steel design guide series 1 - Base plate and anchor rod design, American Institute of Steel Construction, Chicago, 2006.

[3] CEN, Eurocode 3: Design of steel structures, EN 1993, Brussels, 2003.

[4] SCI/BCSA Connections Group, Joints in steel construction: Moment-resisting joints to Eurocode 3 (P398), The Steel Construction Institute and The British Constructional

Steelwork Association, London, 2013.

[5] H. de Clerq, S. Erling, A. Gebremeskel, The Green Book: Structural Steel Connections, South African Institute of Steel Construction, Johannesburg, 2012.

[6] SABS, The structural use of steel (SANS 10162-1), The South African Bureau of Standards, Pretoria, 2011.

[7] P.M. Amaral, Steel Column Bases under Biaxial Loading Conditions, Master's thesis. University of Porto, 2014.

[8] R. Cloete, C. Roth, Column base connections subjected to axial compression and biaxial moments I – experimental and analytical investigation, submitted to Journal of Constructional Steel Research

[9] R. Cloete, Behaviour and design of unstiffened steel column base connections under uniaxial and biaxial bending, PhD thesis, University of Pretoria, 2017.

[10] J. Choi, K. Ohi, Evaluation on interaction surface of plastic resistance for exposed-type steel column bases under biaxial bending, Journal of Mechanical Science and Technology 19(3) (2005) 826–835.

[11] R.M. Drake, S.J. Elkin, Beam-column base plate design-LRFD method, Engineering Journal 36(1) (1999) 29–38.

[12] J.M. Doyle, J.M. Fisher, Discussion: Beam-column base plate design, Engineering Journal 36(1) (1999) 273–274.

[13] G.N. Stamatopoulos, J. Ermopoulos, Interaction curves for column base-plate connections, Journal of Constructional Steel Research 44(97) (1997) 69–89.

[14] D.-Y. Lee, S.C. Goel, B. Stojadinovic, Exposed column-base plate connections bending about weak axis: I Numerical parametric study, International Journal of Steel Structures 8(1) (2008) 11-27.

[15] D.-Y. Lee, B. Stojadinovic, Exposed column-base plate connections bending about weak axis: II Experimental study, International Journal of Steel Structures 8(1) (2008) 29-41.

[16] D. Lee, Seismic behavior of column-base plate connections bending about weak axis, PhD thesis, University of Michigan, 2001.

[17] I.R. Gomez, A. Kanvinde, G.G. Deierlein, Flexural response of exposed column base plate connections, in: Proceedings of the Third International Conference on Advances in Experimental Structural Engineering, San Francisco, 2009, pp. 5–10.

[18] N. Hawkins, The bearing strength of concrete loaded through flexible plates, Magazine of Concrete Research 20(63) (1968) 95–102.

[19] R. Ince, E. Arici, Size effect in bearing strength of concrete cubes, Construction and Building Materials 18(8) (2004) 603–609.

[20] I.R. Gomez, Behavior and design of column base connections, PhD thesis, University of California, 2010.

[21] N.A. Kennedy, S. Vinnakota, A.N. Sherbourne, The split-tee analogy in bolted splices and beam-column connections, in Joints in Structural Steelwork, John Wiley & Sons, London-Toronto, 1981, pp. 2.138-2.157.

[22] A. Wheeler, M. Clarke, G. Hancock, T. Murray, Design model for bolted moment end plate connections joining rectangular hollow sections, Journal of Structural Engineering 124(2) (1998) 164–173.

[23] J. Packer, L. Bruno, P. Birkemoe, Limit analysis of bolted RHS flange plate joints, Journal of Structural Engineering 115(9) (1989) 2226–2242.

[24] J. Ermopoulos, G.N. Stamatopoulos, Mathematical modelling of column base plate connections, Journal of Constructional Steel Research 36(2) (1996) 79–100.

[25] ACI Committee 318, Building Code Requirements for Structural Concrete (ACI 318M-11) and Commentary, American Concrete Institute, Farmington Hills, 2011.